

# The Metric Backbone in the Human Connectome and across Lifespan

Andreia Sofia Teixeira<sup>1,2,3</sup>, Joshua Faskowitz<sup>4,5</sup>, Olaf Sporns<sup>2,4,5</sup>, and Luis M. Rocha<sup>1,2,6</sup>

<sup>1</sup> Center for Social and Biomedical Complexity, School of Informatics, Computing, & Engineering, Indiana University, Bloomington IN, USA

<sup>2</sup> Indiana University Network Science Institute, Indiana University, Bloomington IN, USA

<sup>3</sup> INESC-ID, Lisboa, Portugal

<sup>4</sup> Department of Psychological and Brain Sciences, Indiana University, Bloomington IN, USA

<sup>5</sup> Program in Neuroscience, Indiana University, Bloomington IN, USA

<sup>6</sup> Instituto Gulbenkian de Ciência, Oeiras, Portugal

anmont@iu.edu

## 1 Introduction

Network backbones have been widely used to study the core structure and dynamics of different complex systems, including brain networks [8]. Another key component of network studies is the concept of shortest path, which plays an important role in the optimization of communication. Here we present a preliminary study of the metric backbone – the invariant sub-graph under distance closure that contains all edges that contribute to any shortest path [7, 1] – in human brain structural connectivity of two different cohorts: the Human Connectome Project (HCP) [3] and the Nathan Kline Institute study (NKI) [5]. The HCP is a high-quality dataset of healthy young adults and the NKI provides a community sample with a wide age range, which enables us to track data trends across the lifespan. Ours is the first study of the metric backbone of human connectome networks. Our preliminary results show that it comprises a surprisingly small subgraph of the original networks, that its size decreases in the earlier decades of human life, and that it accounts for a significantly outsized proportion of brain connection cost.

## 2 Building Structural Connectivity Networks

To estimate structural connectivity for each subject in each dataset, diffusion magnetic resonance images were preprocessed, resulting in maps of white matter tract orientation [9]. Probabilistic tractography [2] was performed on these maps, rendering streamline estimates of white matter anatomical architecture. Structural connectivity was measured by counting the streamlines between brain regions, and normalizing for region volume. Using an atlas with 200 functionally-associated regions [6] resulted in a structural connectivity matrix with 200 nodes.

### 3 Extracting the Metric-Backbone

Following [7, 1], we compute the Metric-Backbone as the invariant subgraph under distance closure, which is sufficient to compute all shortest paths. It contains all metric edges of an original distance (or weighted) graph. An edge is metric if it is the shortest distance between its two nodes, otherwise it is semi-metric because it breaks the triangle inequality – there is a shorter distance between the nodes via an indirect path. A simple  $s$  parameter allows us to discriminate these edges:

$$s(e_{ij}) = \frac{e_{ij}}{p(i, j)} \quad (1)$$

where  $e_{ij}$  denotes the (distance) weight of the edge between nodes  $i$  and  $j$  (the direct distance between nodes), and  $p(i, j)$  is the shortest distance path between the same nodes (the smallest sum of distance weights on a path between  $i$  and  $j$ ). To obtain  $p(i, j)$  for all edges we compute the all-pairs shortest path (APSP) problem. Edges with  $s = 1$  define the metric backbone (they are invariant to distance closure [7]) and are sufficient to compute any shortest path in original graph. Edges with  $s > 1$  are semi-metric and do not contribute to any shortest path. Moreover,  $s$  can vary widely for edges not on the backbone, and characterizes how much they break the triangle inequality. For example, the pairs of nodes with  $s_{i,j} > 2$  means that at least one indirect path between  $i$  and  $j$  is at least half as short as the direct distance between these nodes.

The brain structural connectivity adjacency matrices entries denote a proximity between nodes. To calculate the shortest paths as above we convert proximity to distance via the nonlinear transformation  $\frac{1}{x} - 1$ , after normalizing to the interval  $[0, 1]$  as suggested in [7].

### 4 Preliminary Results and Discussion

We study the characteristics of the metric backbone first in the adult HCP cohort, and then compare the same network measures across the lifespan, in the NKI cohort. In this preliminary work we present the results for the fraction of edges in the metric-backbone and the fraction of the connection cost – here defined as the product of the length of the streamline and the streamline count [4] – that it covers. In Figure 1 upper left panel we present the distribution of the fraction of edges in the metric-backbone for the HCP dataset, while in the upper right panel we present the same measurement across the lifespan in the NKI data. The analysis reveals that the metric backbone is comprised of very small subgraph of the original network – around 10 – 13%. In other words, there is a lot of redundancy in these connectome networks, whereby only 10 – 13% are needed to compute all shortest paths. Moreover, in the NKI dataset we observe a significant decline in the size of the backbone in the first three decades (Spearman correlation  $\rho = -0.374$  and  $p\text{-value} = 1.929e^{-08}$ ). For the remaining lifespan there is no evidence of any strong trend correlated with age ( $\rho = -0.063$  and  $p\text{-value} = 0.299$ ), that is, the size of the backbone stabilizes after the first decades.

Interestingly, even though the metric-backbone comprises only a small fraction of edges ( $\approx 11\%$ ), on average, it accounts for about half of the total connection cost. This

suggests that the metric backbone represents a significant “investment” in connecting streamlines and thus that shortest paths are important for communication in brain networks. Our results are validated by null models constructed from a population of 1000 random connected subgraphs of the same original networks.

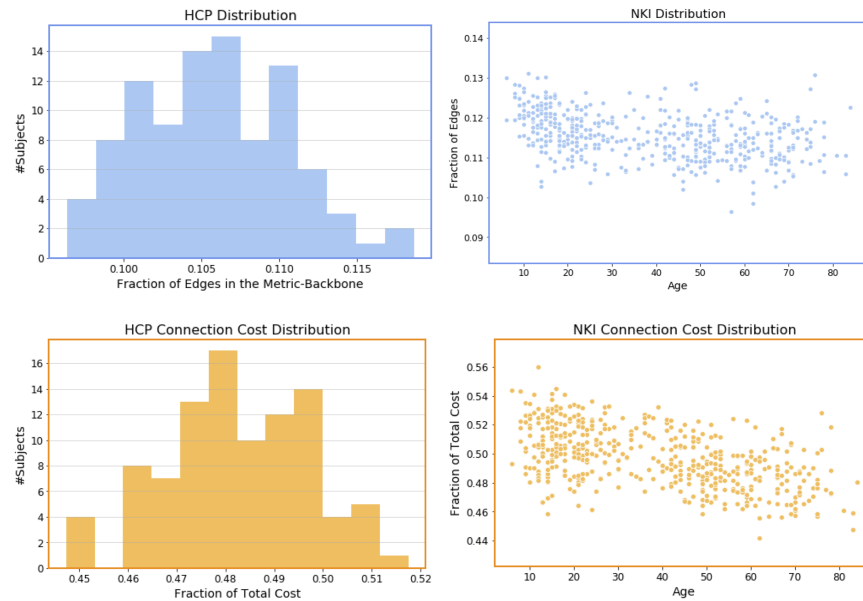


**Fig. 1.** Characteristics of the metric-backbones regarding the fraction of edges that they contain and the fraction of connection cost that they support when comparing with the full networks. Left panel corresponds to the HCP dataset, and the right panel to the NKI dataset.

## References

1. Brattig Correia, R., Barrat, A., Rocha, L.M.: The metric backbone preserves community structure and is a primary transmission subgraph of contact networks in epidemicspread models. Under Review (2020)
2. Garyfallidis, E., Brett, M., Amirbekian, B., Rokem, A., Van Der Walt, S., Descoteaux, M., Nimmo-Smith, I.: Dipy, a library for the analysis of diffusion mri data. *Frontiers in neuroinformatics* 8, 8 (2014)
3. Glasser, M.F., Sotiropoulos, S.N., Wilson, J.A., Coalson, T.S., Fischl, B., Andersson, J.L., Xu, J., Jbabdi, S., Webster, M., Polimeni, J.R., et al.: The minimal preprocessing pipelines for the human connectome project. *Neuroimage* 80, 105–124 (2013)
4. van den Heuvel, M.P., Kahn, R.S., Goñi, J., Sporns, O.: High-cost, high-capacity backbone for global brain communication. *Proceedings of the National Academy of Sciences* 109(28), 11372–11377 (2012)
5. Nooner, K.B., Colcombe, S., Tobe, R., Mennes, M., Benedict, M., Moreno, A., Panek, L., Brown, S., Zavitz, S., Li, Q., et al.: The nki-rockland sample: a model for accelerating the pace of discovery science in psychiatry. *Frontiers in neuroscience* 6, 152 (2012)

6. Schaefer, A., Kong, R., Gordon, E.M., Laumann, T.O., Zuo, X.N., Holmes, A.J., Eickhoff, S.B., Yeo, B.T.: Local-global parcellation of the human cerebral cortex from intrinsic functional connectivity mri. *Cerebral cortex* 28(9), 3095–3114 (2018)
7. Simas, T., Rocha, L.M.: Distance closures on complex networks. *Network Science* 3(2), 227–268 (2015)
8. Sporns, O., Tononi, G., Kötter, R.: The human connectome: a structural description of the human brain. *PLoS Comput Biol* 1(4), e42 (2005)
9. Tournier, J.D., Yeh, C.H., Calamante, F., Cho, K.H., Connelly, A., Lin, C.P.: Resolving crossing fibres using constrained spherical deconvolution: validation using diffusion-weighted imaging phantom data. *Neuroimage* 42(2), 617–625 (2008)